Supporting Information

Construction of imine-hydrazone dual linkages covalent organic frameworks

Yubao Lan,[#] Yufeng Gong,[#] Xiaoya Pang, Yanjun Feng, Yi Ran, Huixia Guo, Xiaoquan Lu*

Key Laboratory of Water Security and Water Environment Protection in Plateau Intersection (Ministry of Education), Key Laboratory of Bioelectrochemistry and Environmental Analysis of Gansu Province, College of Chemistry and Chemical Engineering, Northwest Normal University, Lanzhou 730070, P. R. China.
E-mail: luxq@nwnu.edu.cn
# Yubao Lan and Yufeng Gong contributed equally.

A. General Information

Reagents

All reagents and solvents were obtained from commercial sources and used as received. 1,3,5-Triformylbenzene (TFB), 1,3,5-tri(4-formylphenyl)benzene (TFPB), 4',4''',4'''''',4''''''''-(ethene-1,1,2,2-tetrayl)tetrakis (([1,1'-biphenyl]-4-carbaldehyde)) (ETTTA) were obtained from Jilin Chinese Academy of Sciences Yanshen Technology Co., Ltd. Methyl 2-methoxy-4-aminobenzoate, tetracycline hydrochloride (TC), tetrahydrofuran (THF), 1,4-dioxane, mesitylene and sulfamethoxazole (SMZ) were obtained from Energy Chemical. AcOH was obtained from Shanghai Macklin Biochemical Co., Ltd. Roxithromycin (RXM), sulfadiazine (SD), ampicillin (AMP) and *L*-Histidine (*L*-His) were obtained from Beijing InnoChem Science & Technology Co., Ltd. *L*-Cysteine (*L*-Cys) and *L*-Valine (*L*-Val) were obtained from Shanghai Titan Scientific Co., Ltd. Sodium chloride (NaCl), potassium chloride (KCl) and calcium chloride ($CaCl_2$) were obtained from Shanghai Hushi Laboratorial Equipment Co., Ltd. KBr was obtained from Alab (Shanghai) Chemical Technology Co., Ltd.

Fluorescent measurements

Disperse 3.0 mg DL-COF-44 in 3 mL DMF with the assistance via ultrasonic (30 min). Take DL-COF-44 stock solution (40 μL) and different concentrations of TC were loaded into several centrifugal tubes (2.0 mL) and diluted to 2 mL with DMF. After 1 min of ultrasound, the fluorescence changes of each system were monitored under 323 nm excitation in a quartz test tube at 25 °C.

Instruments and sample preparation

FT-IR spectra were recorded on a Nicolet NEXUS 670 instrument by using KBr pellet.

Powder X-ray diffraction (PXRD) data were collected on a Rigaku-binary diffractometer operated at 40 kV and 40 mA with Cu Kα radiation (step size of 0.017° and step time of 1 s).

Fluorescence spectra were recorded at room temperature using Edinburgh FS5 and Edinburgh FLS1000 combined fluorescence lifetime & steady state spectrometer.

Solid-state NMR experiments were performed on a Bruker WB Avance II 400 MHz spectrometer. Solid-state ^{13}C cross-polarization magic-angle spinning (^{13}C CP/MAS NMR) spectra were recorded with a 4-mm double-resonance MAS probe; a sample spinning rate of 10.0 kHz, a contact time of 3 ms (ramp 100), and a pulse delay of 3 s were applied.

Field emission scanning electron microscopy (SEM) observations were performed on a Hitachi S-4800 microscope operated at an accelerating voltage of 5.0 kV.

The thermal properties of COF samples were evaluated with a STA PT1600 Linseis thermogravimetric analysis (TGA) instrument over the temperature range of 25 to 800 °C under nitrogen atmosphere with a heating rate of 10 °C/min.

Nitrogen adsorption and desorption isotherms were recorded at 77 K with a Micromeritics ASAP 2020M system. Prior to the measurement of the sorption isotherm, the samples were degassed for 8 h at 120 °C. Surface areas were calculated using the Brunauer-Emmett-Teller (BET) method. The pore-size-distribution curves were obtained via the non-local density functional theory (NLDFT).

B. Synthesis of Monomer

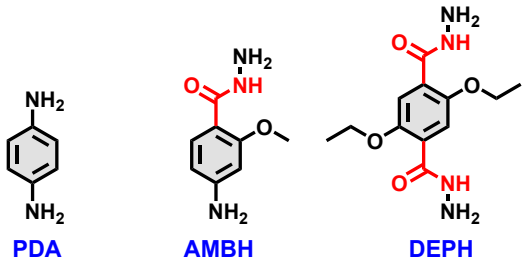

Scheme S1 The chemical structure of building blocks with difference molecule size and functional groups.

Synthesis of AMBH

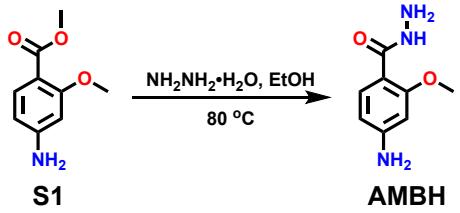

Scheme S2 Synthetic route of **AMBH**.

4-amino-2-methoxybenzohydrazide (AMBH)

Methyl 4-amino-2-methoxybenzoate **S1** (5.0 g, 27.6 mmol) was dissolved in EtOH (50 mL) in a 100 mL round bottom flask equipped with a stir bar. Hydrazine hydrate (10.0 mL, 205 mmol) was added and the flask was then equipped with a condenser and heated to reflux for 48 h. The reaction was then allowed to cool to room temperature, and a while precipitate formed. The flask was then placed in the freezer for 5.0 h. The white solids were isolated by filtration, washed three times with EtOH, and dried under vacuum. **AMBH** was isolated as white solids (4.25 g, 85%).

AMBH: ^{1}H NMR (400 MHz, DMSO-*d*6) δ = 8.73 (s, 1H), 7.59 (d, J = 8.4, 1H), 6.22 (d, J = 2.0, 1H), 6.19 (dd, J = 8.4, 2.0 Hz, 1H), 5.65 (s, 2H) , 4.31 (s, 2H), 3.80 (s, 3H); **^{13}C NMR (150 MHz, DMSO-*d*6)** δ = 165.3, 158.8, 153.2, 132.3, 108.0, 106.2, 96.0, 55.3. **HRMS (ESI)**: m/z calcd. for $[C_8H_{11}O_2N_3 + H]^+$ 182.0924, found 182.0925.

C. Liquid ^{1}H NMR and ^{13}C NMR Spectra

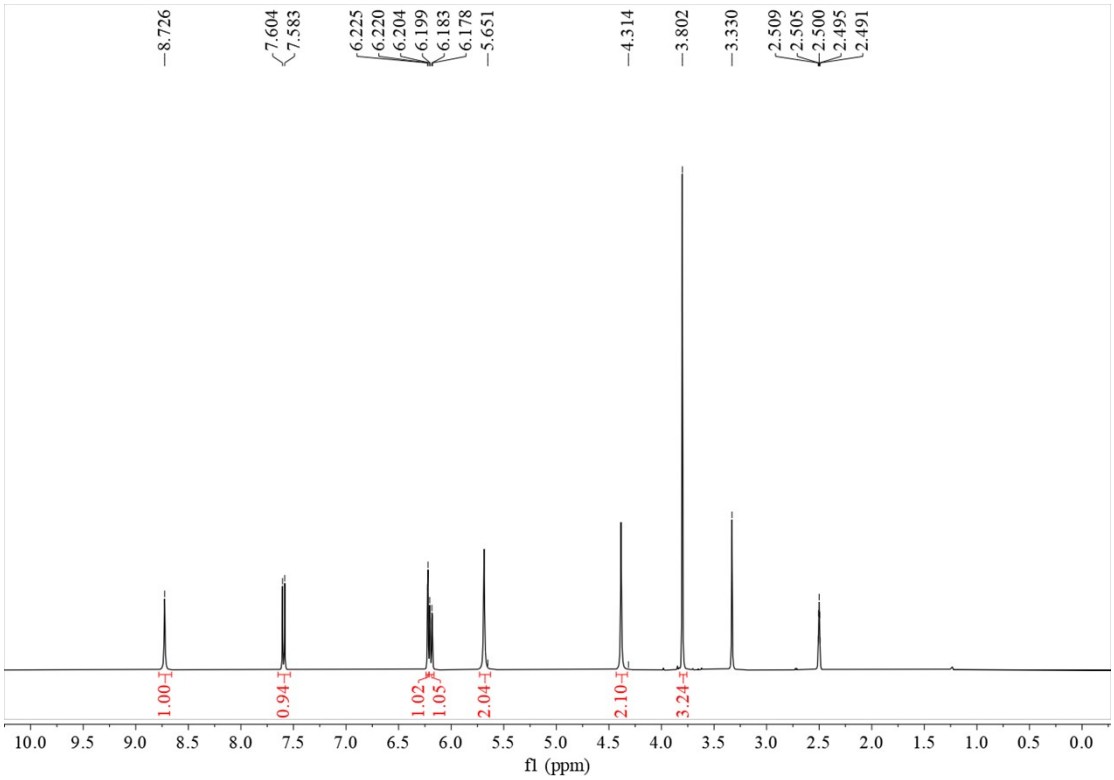

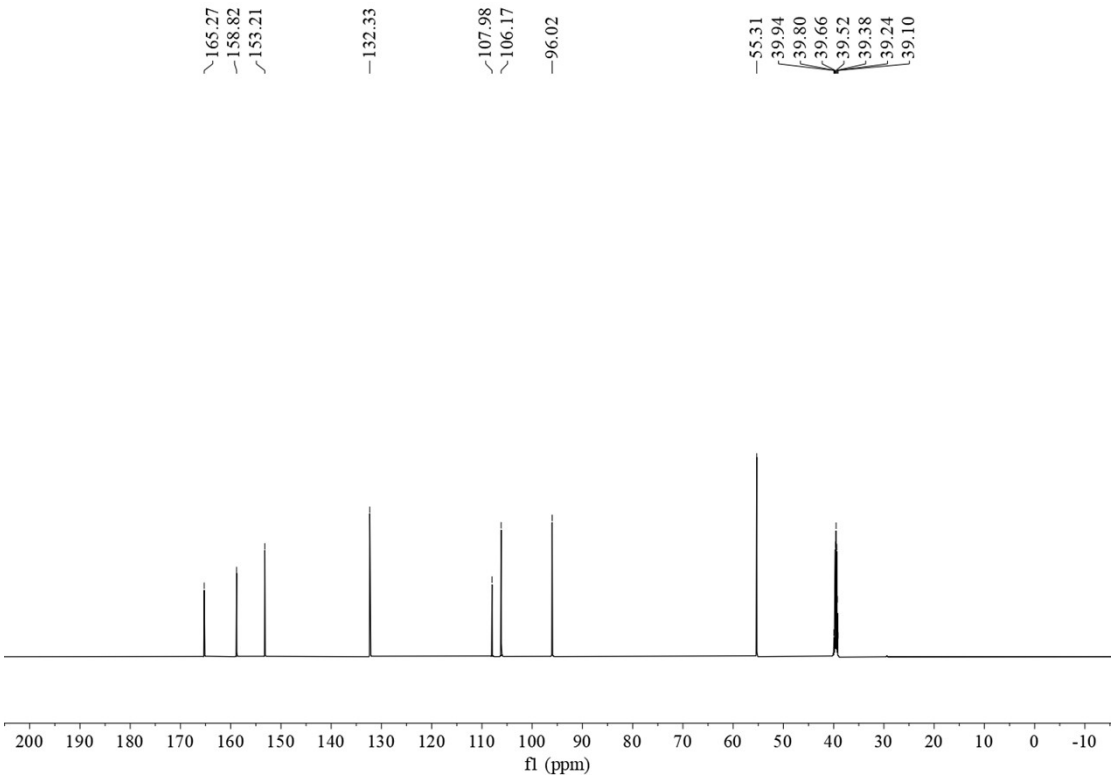

D. Synthesis and Characterization of DL-COF-42

Synthesis of DL-COF-42

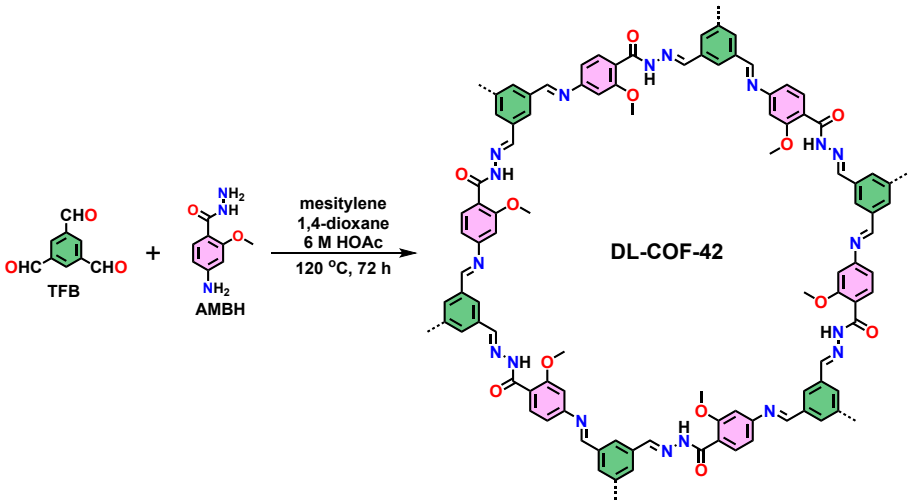

Scheme S3 Synthesis of DL-COF-42 via the condensation of **TFB** and **AMBH**.

To a 15 mL pressure tube were added the **AMBH** (43.5 mg, 0.24 mmol), **TFB** (26.0 mg, 0.16 mmol). Then 1,4-dioxane (0.10 mL) and mesitylene (1.0 mL) were added sequentially. The ampoule was shaken until the slurry was well dispersed. After the dropwise addition of 6 M aqueous acetic acid (0.20 mL), the pressure tube was capped and then placed in an oven at 120 °C for 3 days. The solids were isolated by centrifugation and washed with THF (3 × 5 mL) and acetone (2 × 5 mL). The resulted offwhite solids were dried at room temperature, purified by Soxhlet extraction with THF (24 h). The COF materials were collected and dried at 80 °C for 12 h (85% yield).

Characterization of DL-COF-42

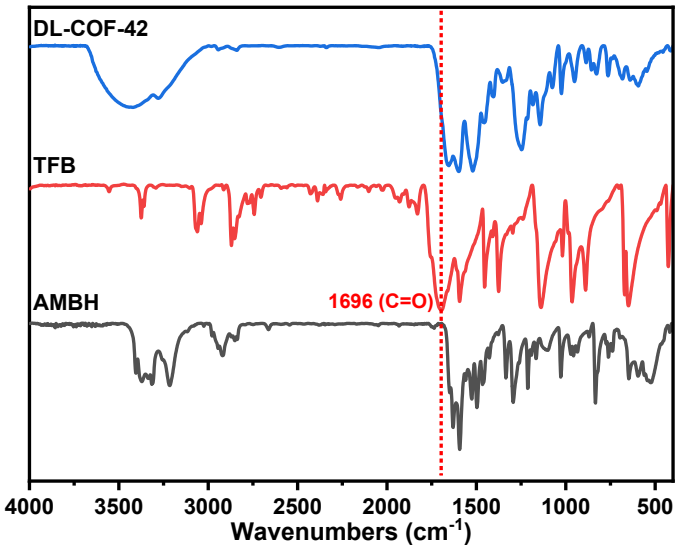

Fig. S1 FT-IR spectra of DL-COF-42 (blue), **TFB** (red) and **AMBH** (black).

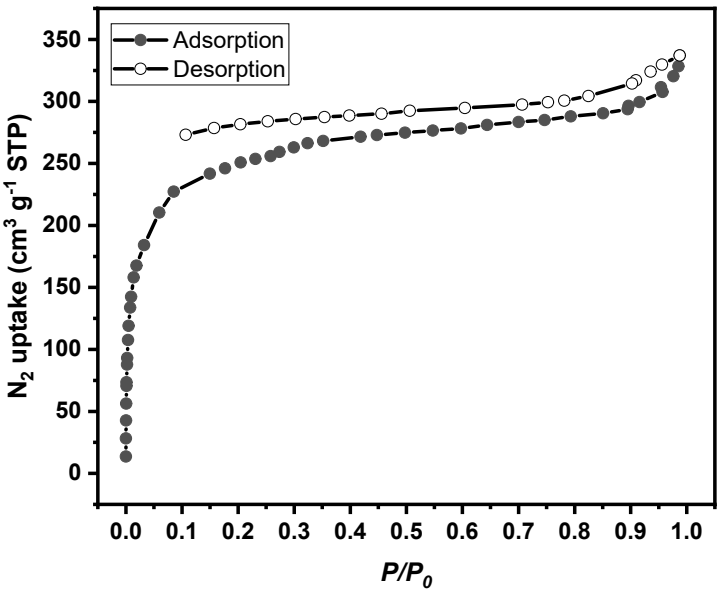

Fig. S2 N_2 adsorption (filled symbols) and desorption (empty symbols) isotherms of DL-COF-42, showing a type-I isotherm characteristic for a microporous structure.

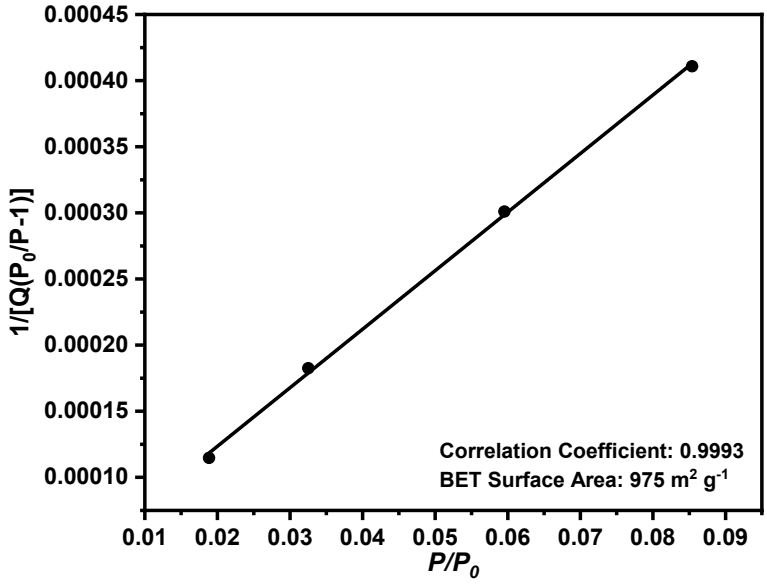

Fig. S3 BET surface area plot for DL-COF-42 calculated from the N_2 adsorption isotherm.

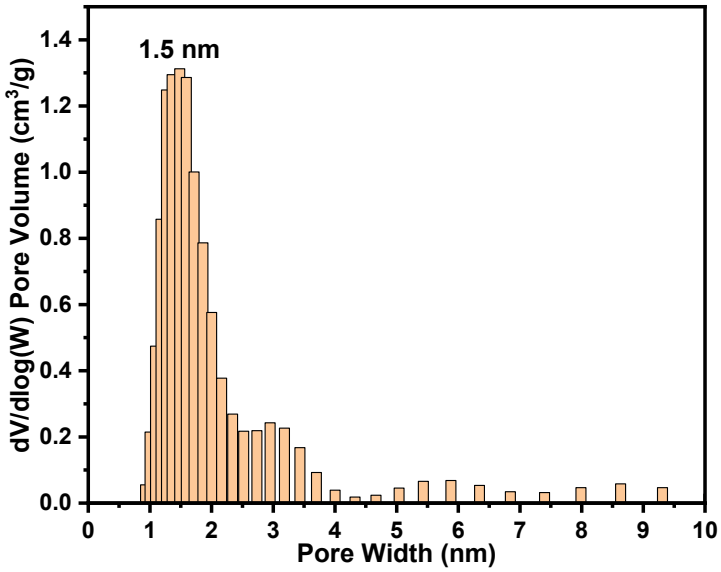

Fig. S4 Pore-size distribution of DL-COF-42 calculated by NLDFT (slit pores model).

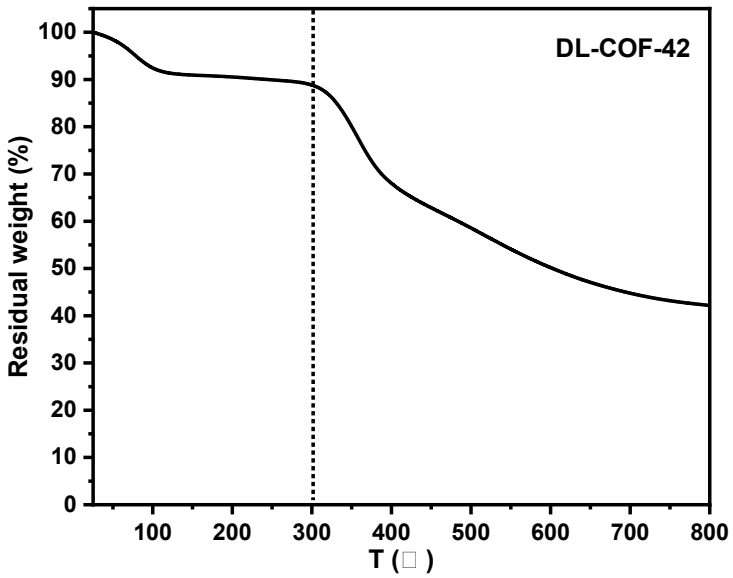

Fig. S5 TGA curve of DL-COF-42, which is thermally stable up to 300 °C.

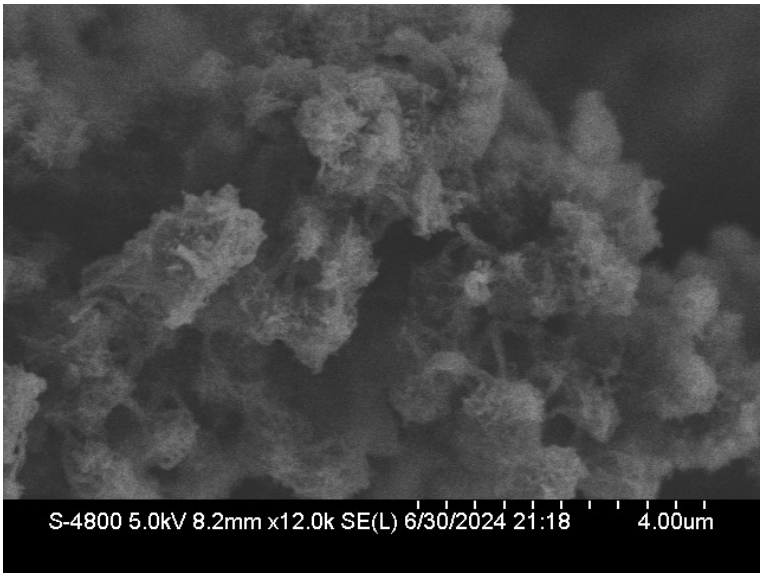

Fig. S6 SEM image of DL-COF-42.

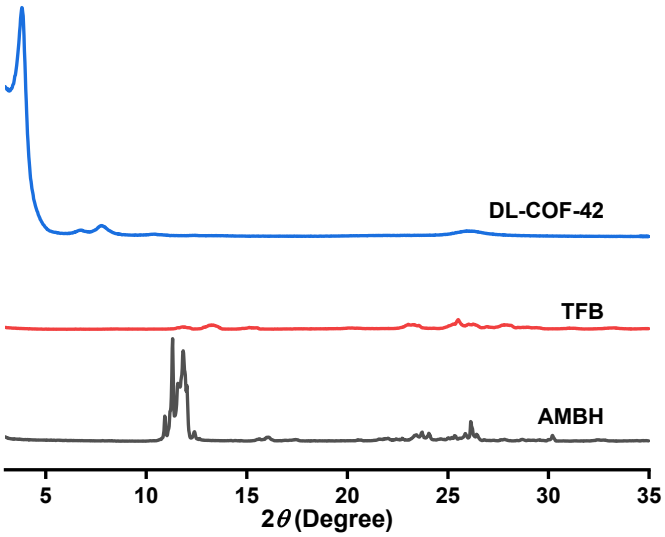

Fig. S7 Comparison of the PXRD patterns of DL-COF-42 (blue), **TFB** (red), and **AMBH** (black).

Structural modeling of DL-COF-42. Structural modeling of DL-COF-42 was generated using the Materials Studio (ver. 8.0) suite of programs. Possible stacking models (eclipsed and staggered) were constructed and optimized using the Forcite module; the calculated PXRD pattern was generated with the Reflex Plus module. Pawley refinement produced the refined PXRD profile with the lattice parameters of $a = b = 25.873$ (± 0.294) Å and $c = 3.686$ (± 0.040) Å. R_{wp} and R_p values converged to 2.78% and 2.16%, respectively. Comparison of the observed and the simulated PXRD patterns (**Fig. S8**) suggested that the preferable structure of DL-COF-42 is the eclipsed arrangement.

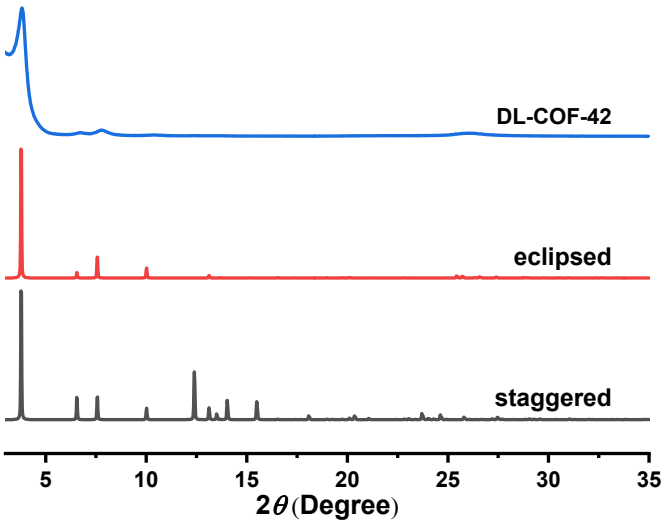

Fig. S8 PXRD patterns of DL-COF-42 observed (blue) and calculated with the

eclipsed (red) and staggered (black) stacking models.

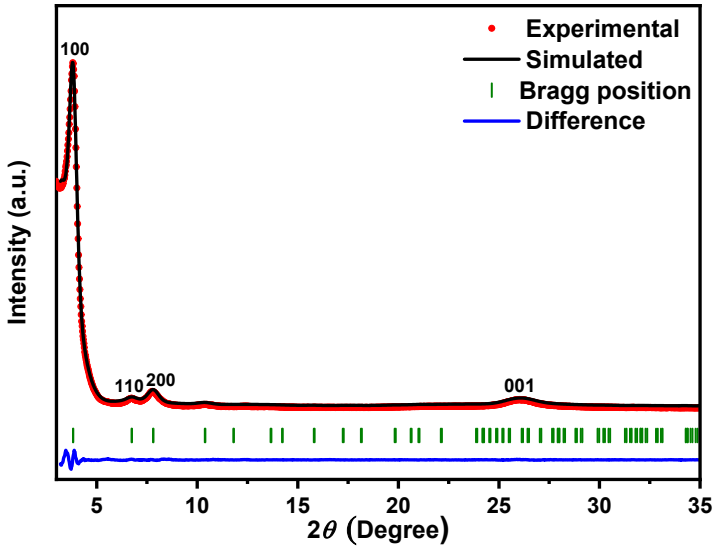

Fig. S9 Pawley refinement for the PXRD pattern of DL-COF-42.

Table S1 Fractional atomic coordinates for the unit cell of DL-COF-42.

DL-COF-42: Space group *P*3							
$a = b = 25.873$ Å, $c = 3.686$ Å $\alpha = \beta = 90.000°$, $\gamma = 120.000°$							
Atom	x	y	z	Atom	x	y	z
C1	2.64881	-0.72519	-0.91594	N16	2.16122	-0.92516	-1.04192
C2	2.6847	-0.60756	-0.91567	C17	2.54572	-0.75184	-0.90258
C3	2.01654	-0.9418	-1.04179	C18	2.12033	-0.91266	-1.03974
C4	1.95791	-0.98329	-1.04174	O19	2.42112	-0.71875	-1.15181
C5	2.40596	-0.76741	-1.04636	H20	2.63489	-0.77045	-0.91168
C6	2.34303	-0.80994	-1.0309	H21	2.02945	-0.89678	-1.04118
C7	2.31996	-0.86906	-1.10423	H22	2.32122	-0.74494	-0.89123
O8	2.35673	-0.88978	-1.2053	H23	2.21869	-0.80889	-0.88183
C9	2.30491	-0.78979	-0.95384	H24	2.24192	-0.95029	-1.1868
C10	2.24559	-0.82668	-0.95182	H25	2.33735	-0.97494	-1.25054
C11	2.22222	-0.88515	-1.03549	H26	2.30907	-0.96013	-0.82986
C12	2.25981	-0.90565	-1.11131	H27	2.38467	-0.93438	-0.8705
C13	2.34588	-0.94225	-1.03013	H28	2.43499	-0.82097	-0.82651
N14	2.44699	-0.78073	-0.94003	H29	2.53398	-0.79591	-0.84704
N15	2.50567	-0.73915	-0.96007	H30	2.13027	-0.86857	-1.04216

E. Synthesis and Characterization of DL-COF-43

Synthesis of DL-COF-43

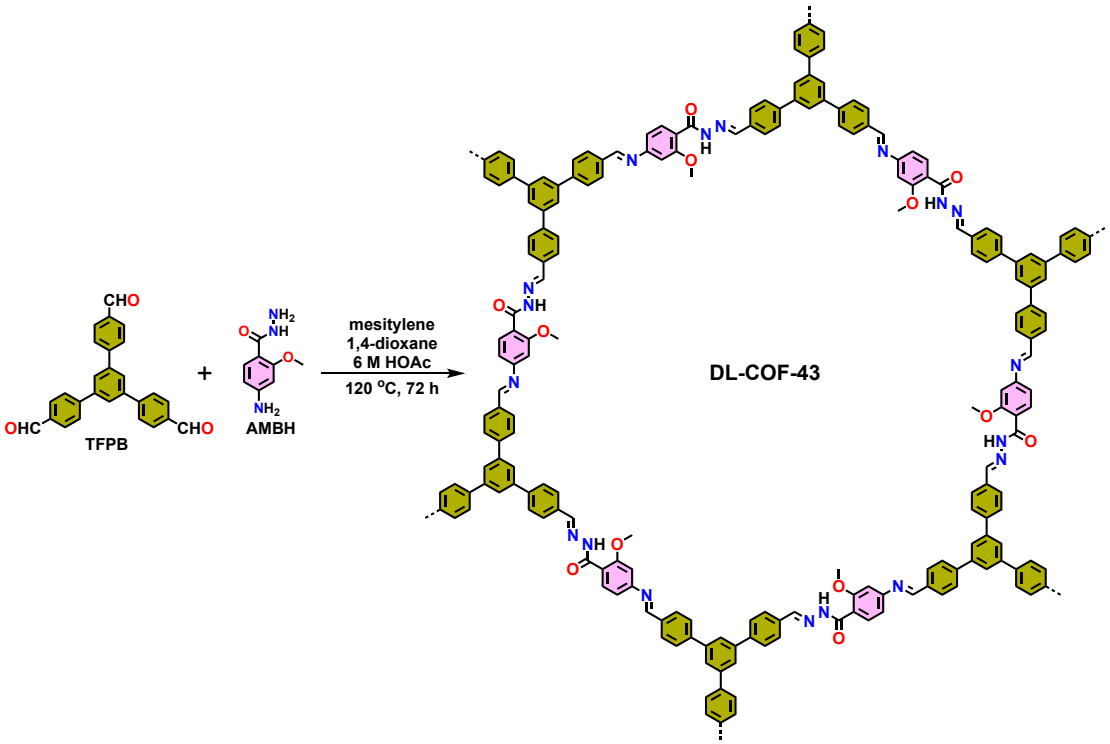

Scheme S4 Synthesis of DL-COF-43 via the condensation of **TFPB** and **AMBH**.

The synthetic procedure of DL-COF-43 was similar to that of DL-COF-42. Condensation of monomer **TFPB** (62.5 mg, 0.16 mmol) and **AMBH** (43.5 mg, 0.24 mmol) afforded DL-COF-43 as a offwhite powder. Further purification of DL-COF-43 was carried out by Soxhlet extraction in THF for 24 h (79% yield).

Characterization of DL-COF-43

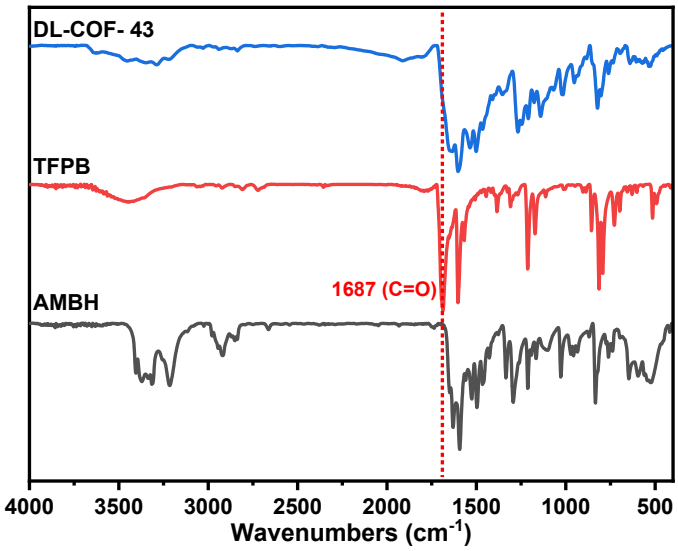

Fig. S10 FT-IR spectra of DL-COF-43 (blue), **TFPB** (red) and **AMBH** (black).

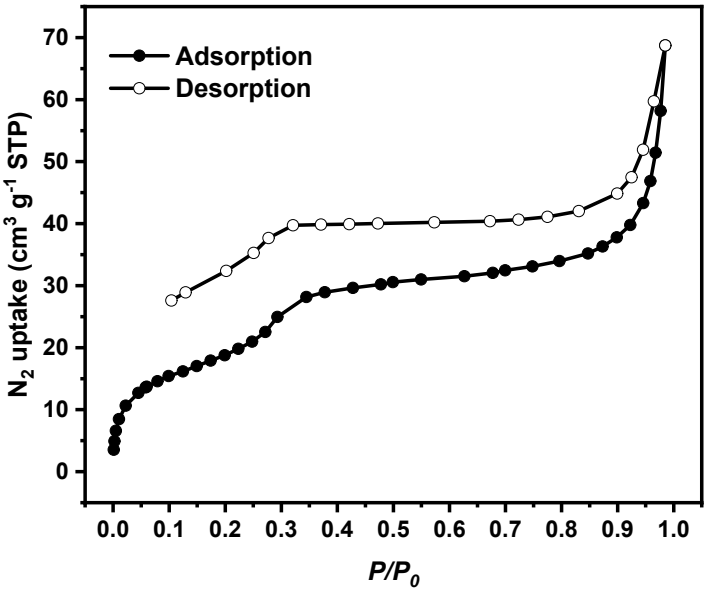

Fig. S11 N_2 adsorption (filled symbols) and desorption (empty symbols) isotherms of DL-COF-43, shows a type-IV isotherm characteristic for a mesoporous structure.

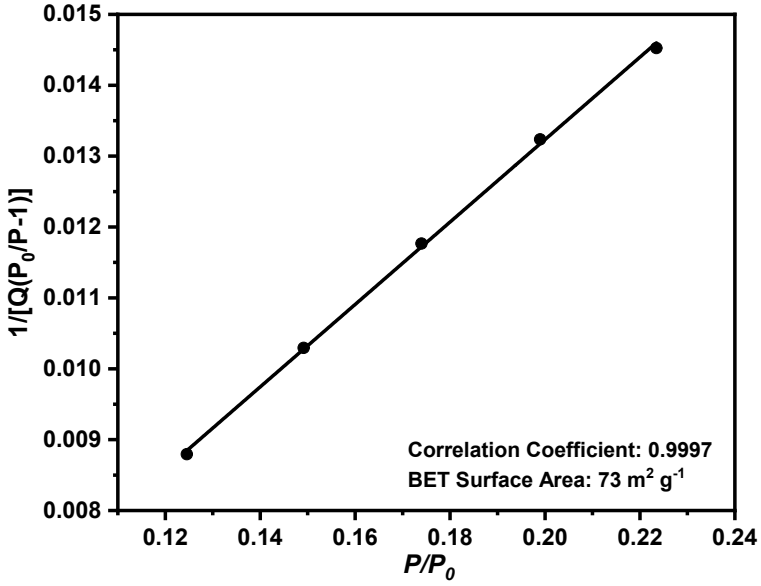

Fig. S12 BET surface area plot for DL-COF-43 calculated from the N_2 adsorption isotherm.

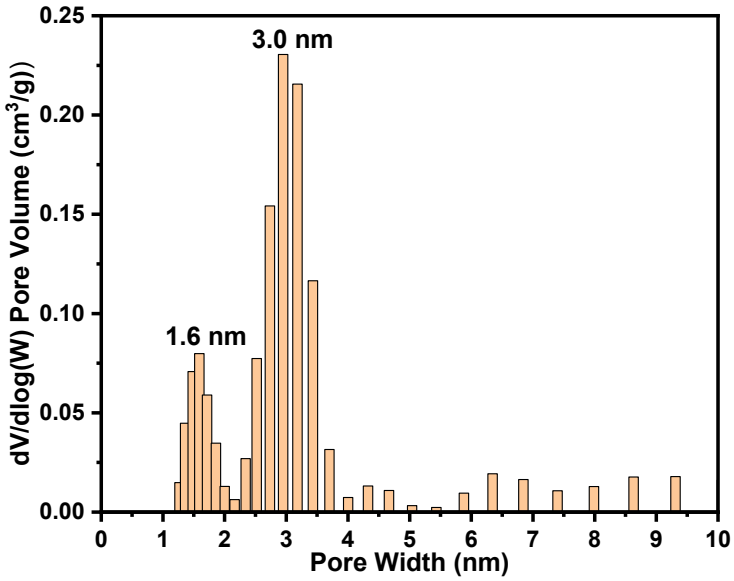

Fig. S13 Pore-size distribution of DL-COF-43 calculated by NLDFT (slit pores model).

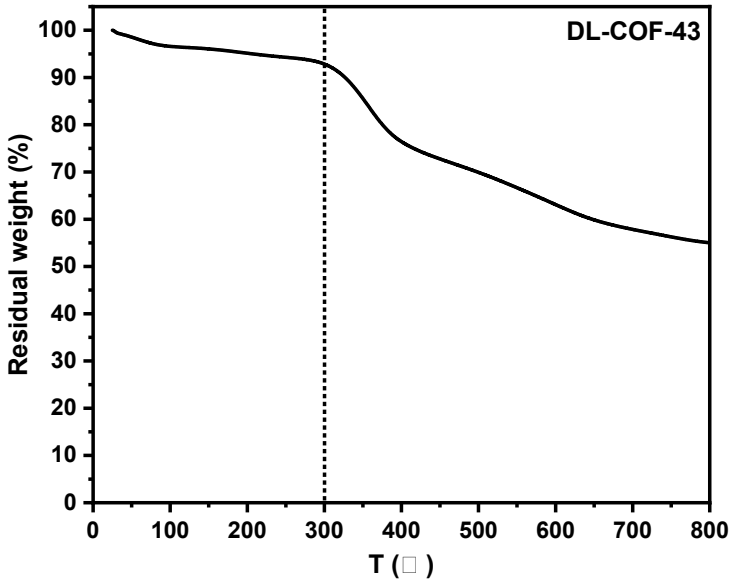

Fig. S14 TGA curve of DL-COF-43, which is thermally stable up to 300 °C.

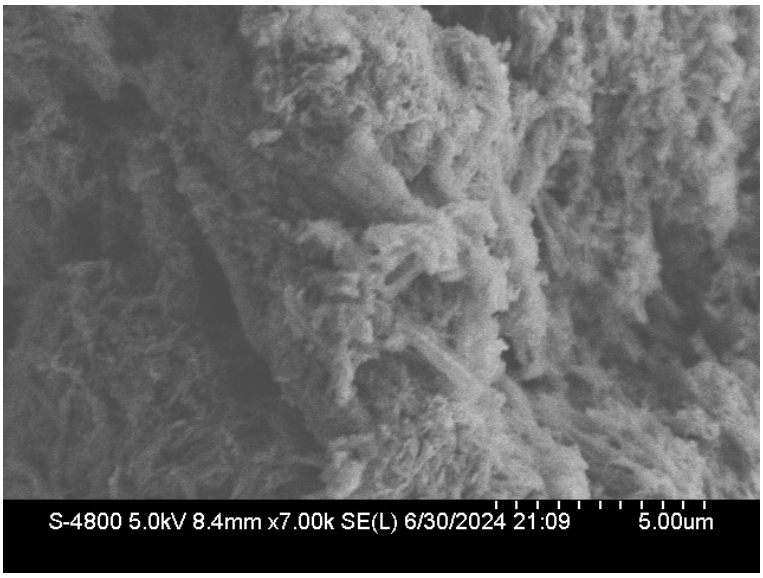

Fig. S15 SEM image of DL-COF-43.

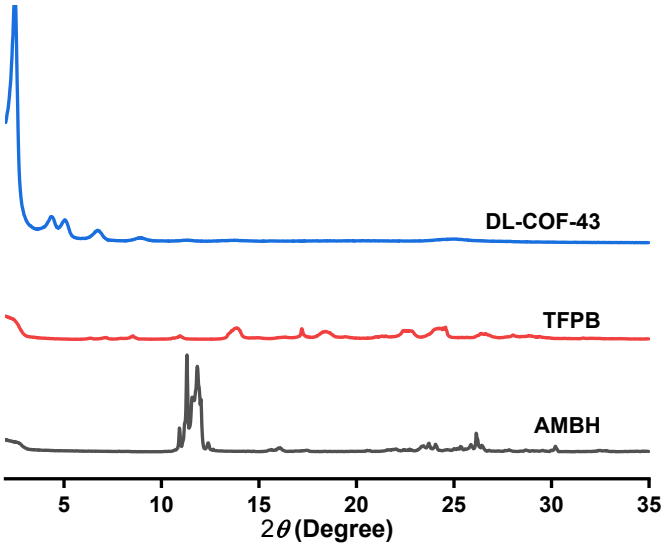

Fig. S16 Comparison of the PXRD patterns of DL-COF-43 (blue), **TFPB** (red), and **AMBH** (black).

Structural modeling of DL-COF-43. Structural modeling of DL-COF-43 was generated using the Materials Studio (ver. 8.0) suite of programs. Possible stacking models (eclipsed and staggered) were constructed and optimized using the Forcite module; the calculated PXRD pattern was generated with the Reflex Plus module. Pawley refinement produced the refined PXRD profile with the lattice parameters of $a = b = 40.470$ (± 0.704) Å and $c = 3.849$ (± 0.064) Å. R_{wp} and R_p values converged to 3.77% and 2.87%, respectively. Comparison of the observed and the simulated PXRD patterns (**Fig. S17**) suggested that the preferable structure of DL-COF-43 is the eclipsed arrangement.

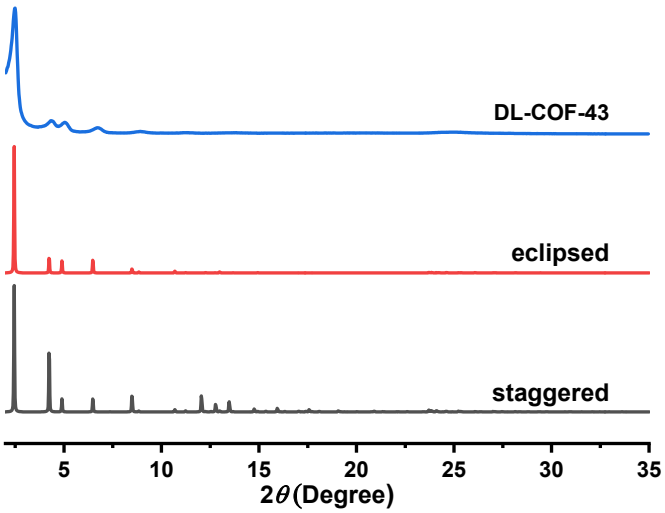

Fig. S17 PXRD patterns of DL-COF-43 observed (blue) and calculated with the

eclipsed (red) and staggered (black) stacking models.

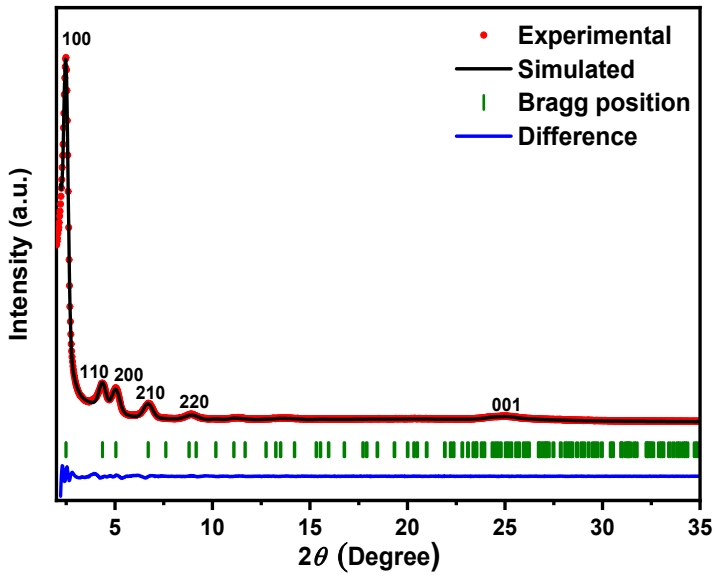

Fig. S18 Pawley refinement for the PXRD pattern of DL-COF-43.

Table S2 Fractional atomic coordinates for the unit cell of DL-COF-43.

DL-COF-43: Space group *P*3							
$a = b = 40.470$ Å, $c = 3.849$ Å $\alpha = \beta = 90.000°$, $\gamma = 120.000°$							
Atom	x	y	z	Atom	x	y	z
C1	1.10383	-0.96506	-0.82852	C23	1.3336	-0.76781	-0.54423
C2	1.14247	-0.94267	-0.83926	N24	1.26065	-0.86905	-0.92668
C3	1.13617	-0.89472	-1.13767	N25	1.22232	-0.89365	-0.91359
C4	1.0976	-0.91741	-1.13592	N26	1.44423	-0.78191	-0.87724
C5	1.08063	-0.95295	-0.97903	C27	1.19948	-0.88256	-1.00448
C6	1.03918	-0.97714	-0.97403	C28	1.15891	-0.90721	-0.99244
C7	1.01605	-0.96145	-0.97338	C29	1.46826	-0.7907	-0.99093
C8	1.53231	-0.77553	-1.132	C30	1.50854	-0.76455	-0.98289
C9	1.57068	-0.7516	-1.13121	O31	1.27503	-0.91438	-0.8105
C10	1.58642	-0.7162	-0.97263	H32	1.02842	-0.9317	-0.9737
C11	1.56219	-0.70552	-0.81983	H33	1.09236	-0.99147	-0.69373
C12	1.52372	-0.72923	-0.82844	H34	1.15941	-0.95279	-0.72053
C13	1.62767	-0.69073	-0.9678	H35	1.14835	-0.86759	-1.26058
C14	1.65199	-0.70504	-0.96712	H36	1.08136	-0.90718	-1.26679
C15	1.28653	-0.88148	-0.86164	H37	1.34007	-0.89657	-1.05216
C16	1.32714	-0.85509	-0.86627	H38	1.40689	-0.85527	-1.06308
C17	1.34222	-0.81761	-0.76325	H39	1.39381	-0.76521	-0.69089
O18	1.31774	-0.80563	-0.64664	H40	1.52109	-0.80253	-1.25591
C19	1.3511	-0.868	-0.97136	H41	1.58775	-0.76074	-1.26386
C20	1.38939	-0.84431	-0.97896	H42	1.57275	-0.67924	-0.6843
C21	1.40483	-0.80702	-0.87811	H43	1.50595	-0.72024	-0.7072
C22	1.38125	-0.79394	-0.7706	H44	1.64067	-0.73467	-0.96731

F. Synthesis and Characterization of DL-COF-44

Synthesis of DL-COF-44

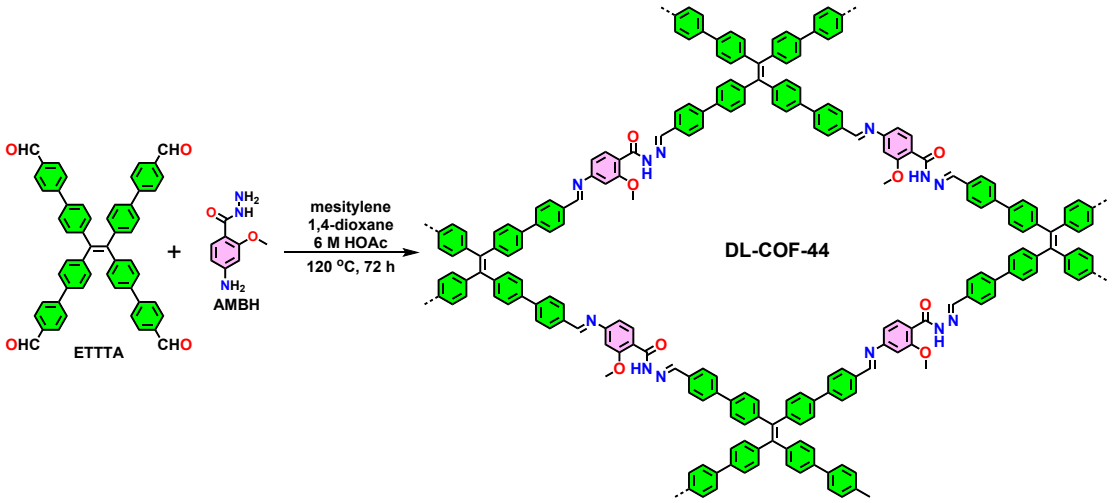

Scheme S5 Synthesis of DL-COF-44 via the condensation of **ETTTA** and **AMBH**.

The synthetic procedure of DL-COF-44 was similar to that of DL-COF-42. Condensation of monomer **ETTTA** (60.0 mg, 0.08 mmol) and **AMBH** (29.0 mg, 0.16 mmol) afforded DL-COF-44 as a yellow powder. Further purification of DL-COF-44 was carried out by Soxhlet extraction in THF for 24 h (74% yield).

Characterization of DL-COF-44

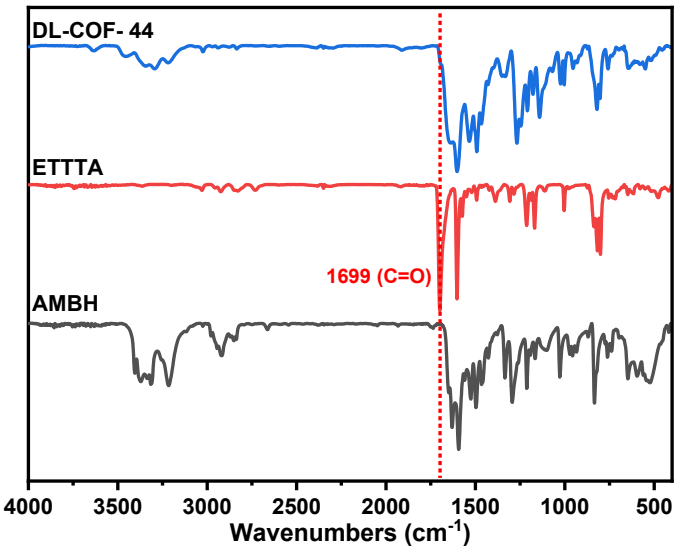

Fig. S19 FT-IR spectra of DL-COF-44 (blue), **ETTTA** (red) and **AMBH** (black).

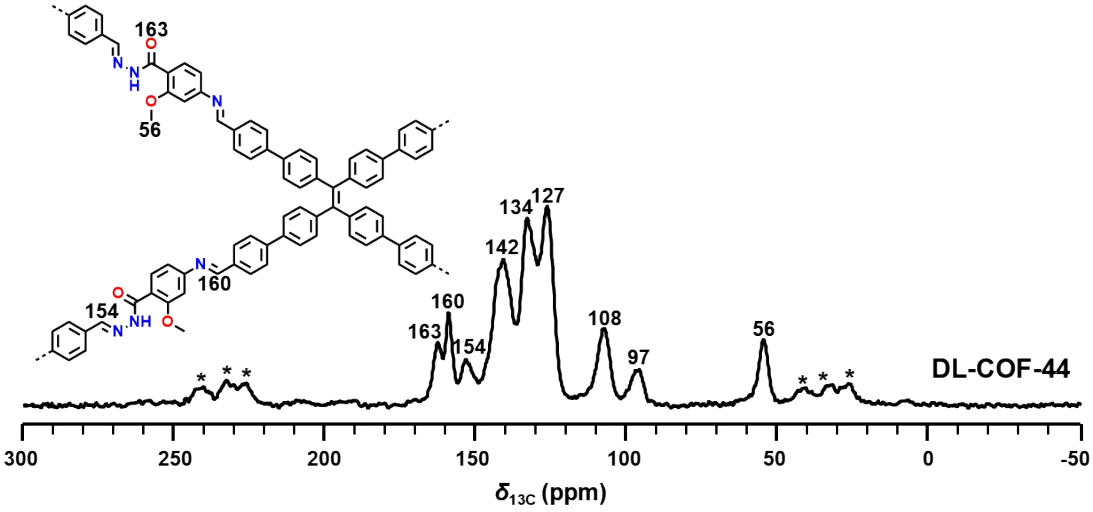

Fig. S20 Solid-state ^{13}C CP/MAS NMR spectrum of DL-COF-44. Asterisks denote the spinning sidebands.

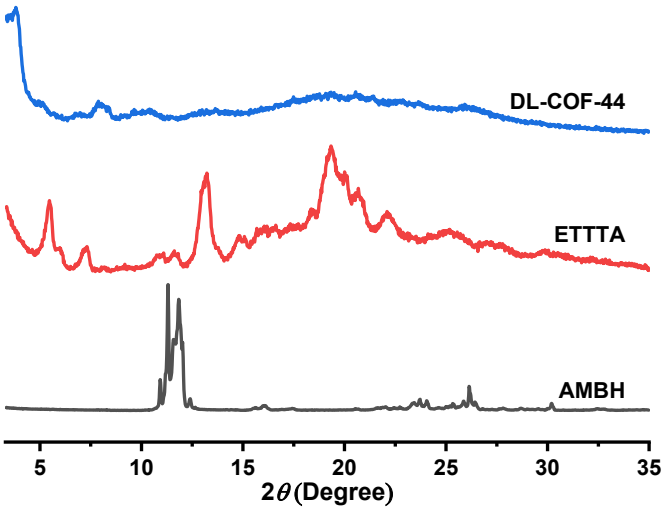

Fig. S21 Comparison of the PXRD patterns of DL-COF-44 (blue), **ETTTA** (red), and **AMBH** (black).

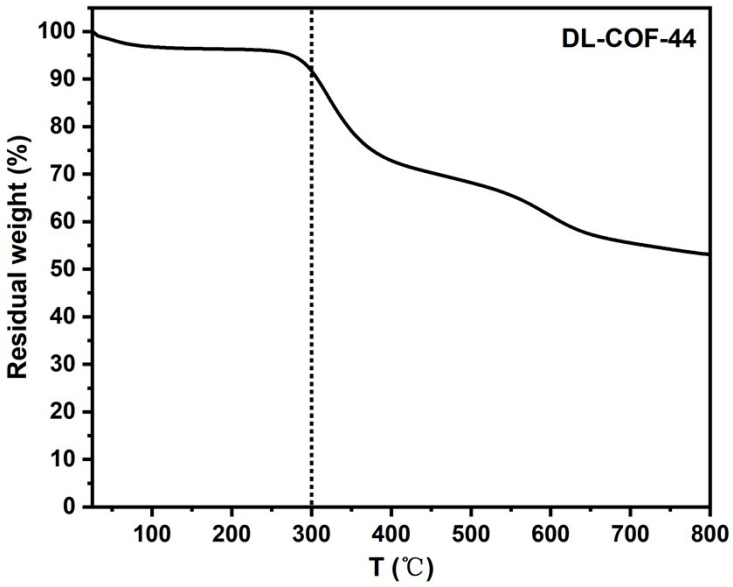

Fig. S22 TGA curve of DL-COF-44, which is thermally stable up to 300 °C.

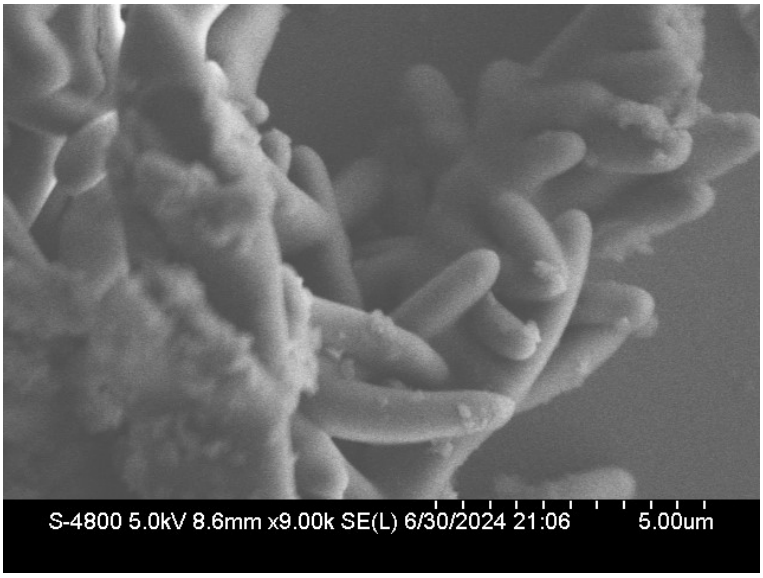

Fig. S23 SEM image of DL-COF-44.

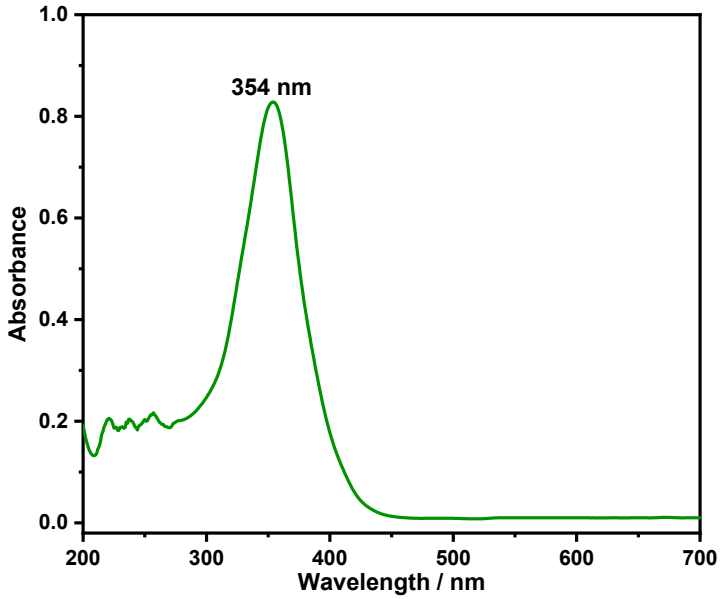

Fig. S24 UV–vis absorption spectrum of the DL-COF-44.

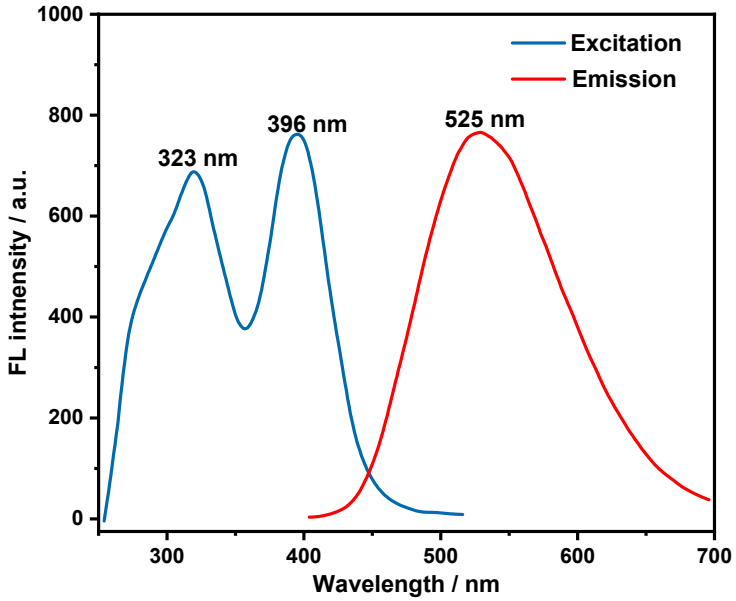

Fig. S25 Fluorescence spectra of DL-COF-44 in DMF (λ_{ex} = 323 nm).

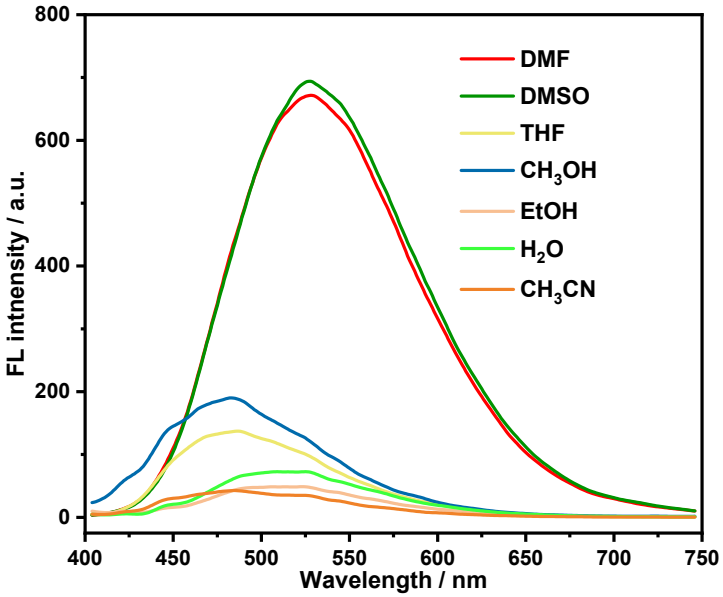

Fig. S26 Fluorescence spectra of DL-COF-44 in different solvents.

G. Fluorescence Detection of TC

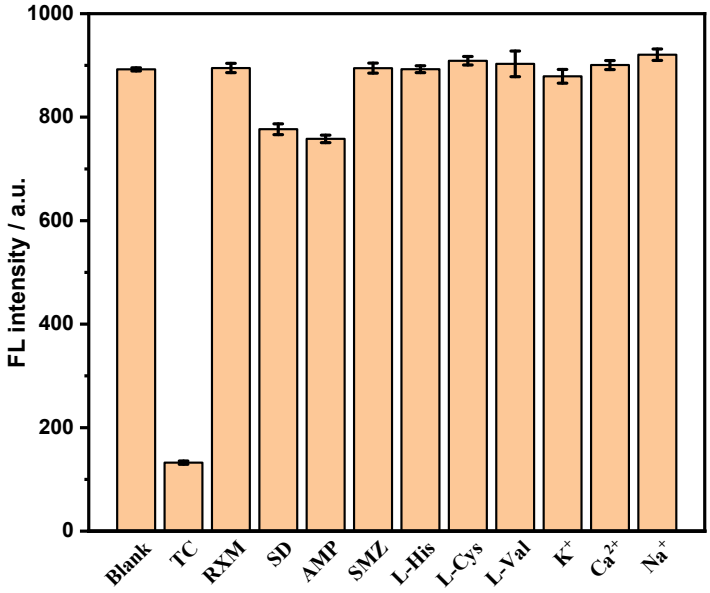

Fig. S27 DL-COF-44 fluorescence sensor (0.02 mg/mL) for responses to TC (60 μM) and other analytes (120 μM) in DMF.

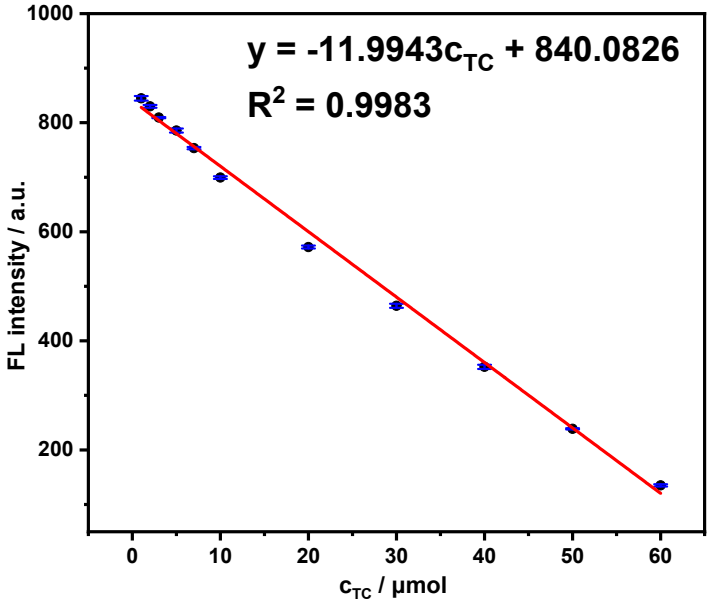

Fig. S28 Linear fitting for the fluorescence intensity data from 0 to 60 μM (R^2 = 0.9983, LOD = 0.404 μM).

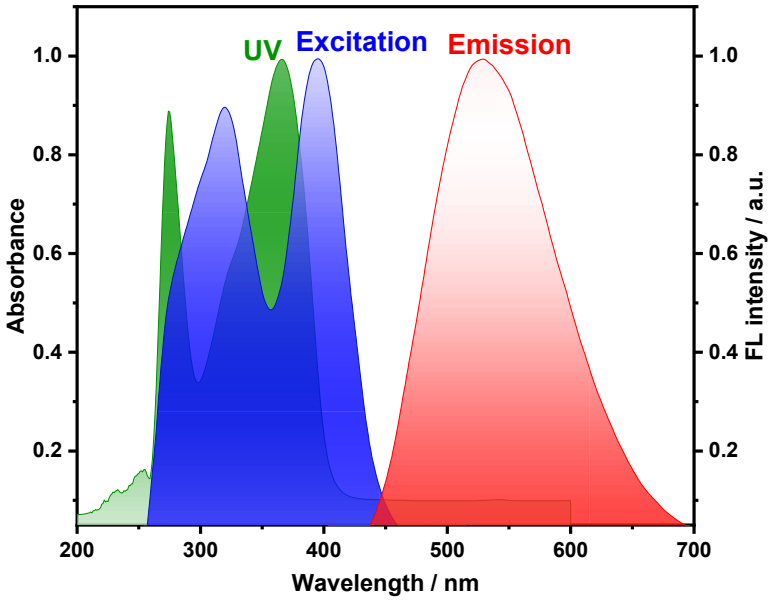

Fig. S29 Normalized UV−vis absorption spectra of TC in DMF and normalized fluorescence excitation and emission spectra of DL-COF-44 in DMF.

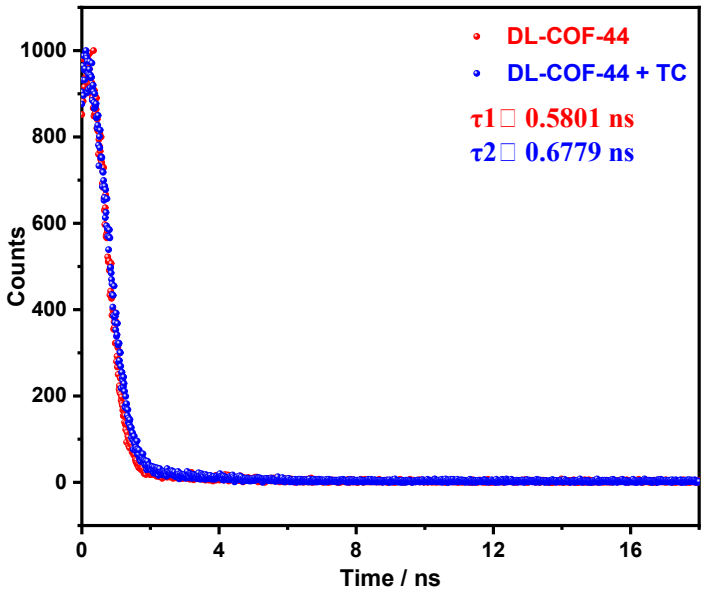

Fig. S30 Comparison of fluorescence lifetime of DL-COF-44 before and after TC addition.